

## Neutron-diffraction study of $\text{ND}_4\text{Cl}$ in the tricritical region\*

W. B. Yelon<sup>†</sup>, D. E. Cox, and P. J. Kortman<sup>†</sup>  
*Brookhaven National Laboratory, Upton, New York 11973*

W. B. Daniels

*University of Delaware, Newark, Delaware 19711*

(Received 15 October 1973)

A detailed neutron scattering investigation has been made of the order-disorder transition in a crystal of  $\text{N}(\text{D}_{0.93}\text{H}_{0.07})_4\text{Cl}$  as a function of both temperature and pressure, with emphasis on the region close to the tricritical point (TCP). At atmospheric pressure, the temperature dependence of the order parameter  $\psi$  was obtained by means of a detailed crystal structural analysis, which revealed that the transition was first order. It was also found that  $\psi$  could be determined with suitable accuracy simply by measuring the intensity of the (221) reflection, which is negligibly small in the disordered region. Intensity data for this reflection were obtained at elevated pressures up to a maximum of 6 kbar both as a function of pressure and temperature, and the phase line was accurately located. This was approximately linear, with an average slope of about 8 °K/kbar. From the behavior of the critical scattering, which showed quite abrupt changes in the disordered region close to the TCP, the latter was determined to lie at  $128 \pm 10$  bar and  $(250.2 \pm 0.1)$  °K. The critical exponents at the TCP were determined for scans made at constant pressure and temperature, and were found to have significantly different values,  $2\beta_c = 0.36 \pm 0.01$  and  $0.28 \pm 0.01$ , respectively. In the second-order region a similar tendency was observed for scans made through a given transition point in these directions. At 280 °K,  $2\beta$  for constant pressure and temperature scans, respectively, had values  $0.61 \pm 0.04$  and  $0.50 \pm 0.04$ , the former being close to the three-dimensional Ising value.

### I. INTRODUCTION

Ammonium chloride undergoes a first-order phase transition at atmospheric pressure in the vicinity of 250 °K from a state in which the hydrogen tetrahedra are disordered to one in which they are oriented in a parallel ("ferromagnetic") arrangement. This transition has been studied by many investigators using various techniques both at atmospheric pressure<sup>1-7</sup> and at elevated pressures.<sup>8-13</sup> At about 1500 bar<sup>11-13</sup> the transition becomes second order and remains so at higher pressures. The point joining the first- and second-order phase lines is a rather special one which has become known as the tricritical point<sup>14</sup> (TCP), and has recently been the subject of considerable interest, both theoretical<sup>14-19</sup> and experimental,<sup>20-24</sup> since a new type of critical behavior is predicted. In particular, an entirely new set of critical indices is expected and the feature of "smoothness"<sup>14</sup> thought to be obeyed along the second-order line is expected to break down at the TCP.

Other systems with tricritical points include  $\text{He}^3$ - $\text{He}^4$  mixtures,<sup>19,23,24</sup> metamagnets such as dysprosium-aluminum-garnet (DAG)<sup>22</sup> and  $\text{FeCl}_2$ <sup>21,25</sup> and the mixed ferroelectric system  $\text{K}(\text{Ta}_x\text{Nb}_{1-x})\text{O}_3$  (KTN).<sup>26</sup> These have been studied to varying degrees, but very little experimental information exists to indicate whether the behavior at the TCP can be thought of as "universal" in some sense, and whether the current models, which are based on simple scaling theory, provide an adequate description.

The present paper describes a careful neutron investigation of the long-range and to a lesser extent the short-range order in  $\text{ND}_4\text{Cl}$  as a function of temperature and pressure, and is arranged in the following format. In Sec. II the sample preparation and the crystallography of  $\text{ND}_4\text{Cl}$  are described. In Sec. III the results of detailed structural studies at atmospheric pressure are presented, including the temperature dependence of the order parameter  $\psi$ , and the order of the transition. The studies performed at elevated pressures are described in Sec. IV. These include the determination of the TCP, and the values of the critical indices in various regions of the phase diagram. Of particular interest are the inequalities in the latter observed for constant pressure and temperature measurements at the same point on the phase lines, and also the low values for  $\beta$  observed at the TCP. Finally, in Sec. V the implication of these results with respect to existing theories of smoothness and tricritical phenomena is discussed.

### II. SAMPLE PREPARATION AND CRYSTALLOGRAPHY

Single crystals of  $\text{ND}_4\text{Cl}$  were grown from an aqueous solution to which about 10% urea had been added in order to promote a cubic growth habit. The starting materials were prepared by deuterating  $\text{NH}_4\text{Cl}$  and normal urea by repeated solution and recrystallization from  $\text{D}_2\text{O}$ . After seven such cycles the solution was placed in a desiccator and allowed to evaporate slowly at room temperature. Seeds were collected and a few returned to the liq-

uid. In this way cubic crystals of up to 5 mm in size with well-defined (100) faces were easily prepared. The crystals which appeared best under visual examination were typically found to have mosaic widths between  $0.20^\circ$  and  $1^\circ$ , and many showed multiple peaks characteristic of low-angle grain boundaries. These imperfections are thought to result from inclusions of urea which cause small shifts in the direction of growth planes.

The degree of deuteration of the samples chosen for study was determined by measuring the average coherent neutron scattering length of the atoms in the deuterium-hydrogen positions and was found to be  $(93 \pm 2)\%$  (see Sec. III). Crystals from the same batch of material were analyzed for urea by wet-chemical techniques but no trace of the latter could be detected within the sensitivity limit of 200 ppm.

Ammonium chloride has the cubic CsCl structure (space group  $Pm\bar{3}m$ , cell edge  $3.87 \text{ \AA}$ ) with essentially rigid tetrahedra of hydrogen or deuterium surrounding the nitrogen atoms.<sup>27</sup> In the disordered phase, above about  $250^\circ\text{K}$ , the four hydrogen atoms are randomly distributed in the  $8(g)$  positions  $(x, x, x)$ , with  $x \sim 0.15$ . These correspond to two equivalent sets of tetrahedral sites lying along the body diagonals of the unit cell (Fig. 1). One of these sets, referred to as the  $[111]$  orientation, has the coordinates  $\vec{r}_H = (x, x, x)$ ,  $(x, \bar{x}, \bar{x})$ ,  $(\bar{x}, x, \bar{x})$ , and  $(\bar{x}, \bar{x}, x)$ , with  $\vec{r}_N = 0, 0, 0$  and  $\vec{r}_{Cl} = \frac{1}{2}, \frac{1}{2}, \frac{1}{2}$ . The alternative orientation, referred to as  $[\bar{1}\bar{1}\bar{1}]$ , consists of inversion through the origin of the four hydrogen positions above.

In the low-temperature phase there are domains in which the tetrahedra are preferentially ordered in one of these orientations, e.g.,  $[111]$ . The system is thought to be well represented by a pseudo-spin- $\frac{1}{2}$  Ising ferromagnet.<sup>12</sup> The space group for the ordered phase is still primitive cubic ( $P\bar{4}3m$ ) so that there are no superlattice lines. As in the case of a simple ferromagnet, the "magnetic" Bragg peaks occur at the same positions as the Bragg peaks for the disordered phase.

### III. STUDIES AT ATMOSPHERIC PRESSURE

#### A. Experimental

Since there are no superlattice peaks, an accurate determination of the order parameter at any

temperature requires a knowledge of the other structural parameters, including the Debye-Waller factors, and the possibility of significant changes in some of these parameters in the vicinity of the transition temperature must be borne in mind. Neutron diffraction studies of the order-disorder transition have previously been reported<sup>27</sup> but these were not of sufficient accuracy to give the information desired. A series of intensity measurements were therefore made at atmospheric pressure as a function of temperature.

The sample chosen for structural studies had dimensions  $2 \times 2 \times 3 \text{ mm}$  and a mosaic width of  $0.2^\circ$ . In order to avoid half-wavelength contamination, the (311) reflection from a Ge monochromator was used, providing incoming neutrons of wavelength  $1.25 \text{ \AA}$ . The collimation in-pile and between monochromator and sample was  $20'$ . The sample was mounted with a  $[110]$  axis vertical, carefully centered and masked, and measurements were made at 15 temperatures between  $230$  and  $255^\circ\text{K}$ . At each temperature 17 reflections of the type  $(hhl)$  were studied. In addition, at several temperatures ten reflections of the type  $(\bar{h}\bar{h}l)$  for  $h \neq 0$  and  $l \neq 0$  were measured and compared for agreement. In all cases this agreement was better than 10% except for the (223) reflection which was so weak that background uncertainties exceeded these errors.

The data at each temperature were fitted by the method of least squares to a simple model without free rotation of the hydrogen tetrahedra.<sup>12,27</sup> The total structure factor is

$$F_T = \psi F_{LT} + (1 - \psi) F_{HT} \quad , \quad (1)$$

where  $F_{LT}$  and  $F_{HT}$  are the structure factors for the low- and high-temperature phases, respectively.  $\psi$ , the order parameter, is defined as

$$\psi = \frac{|N[111] - N[\bar{1}\bar{1}\bar{1}]|}{N[111] + N[\bar{1}\bar{1}\bar{1}]} \quad , \quad (2)$$

where  $N[111]$  and  $N[\bar{1}\bar{1}\bar{1}]$  are the number of tetrahedra having  $[111]$  and  $[\bar{1}\bar{1}\bar{1}]$  orientations, respectively, within a given domain. Above  $T_c$ ,  $\psi$  is expected to be zero, while far below the ordering temperature  $\psi$  should equal one.  $F_{HT}$  allows for the random distribution of tetrahedra by assigning a weight of one-half to each of the eight possible

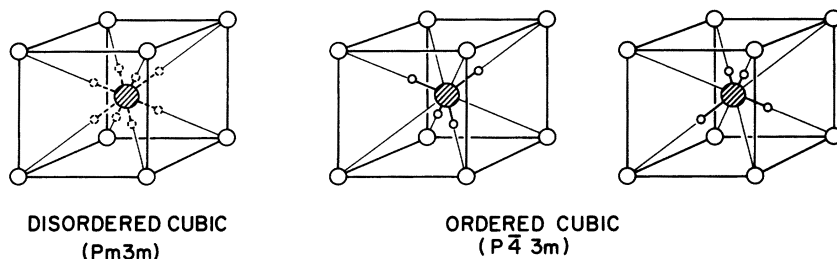


FIG. 1. Crystal structure of  $\text{ND}_4\text{Cl}$ . In the ordered phase, the deuterium tetrahedra are oriented in one of the two equivalent positions shown on the right. In the disordered phase, the tetrahedra are distributed at random as indicated by the broken lines.

deuterium positions in the unit cell,<sup>27</sup> whereas  $F_{LT}$  gives unit weight to the [111] set and zero weight to the  $[\bar{1}\bar{1}\bar{1}]$  set of orientations.

In both the ordered and disordered structures, the Debye-Waller expression takes the same form. The site symmetries of the nitrogen and chlorine atoms permit only isotropic Debye-Waller factors  $B_{11}$ , whereas the local symmetry of the deuterium atoms is lower ( $3m$ ) so that the amplitudes of vibration may be different parallel and perpendicular to the [111] direction, and two Debye-Waller factors are necessary,  $B_{11}$  and  $B_{12}$ .<sup>28</sup>

In addition to these thermal factors and the order parameter, the deuterium positional parameter and scattering length were treated as variables in the structure factor expression. An instrumental scale factor and an extinction coefficient were also included in the refinement, yielding nine parameters in all. The observed intensities were initially corrected for absorption with the assumption of a composition 3% hydrogen and 97% deuterium, and the data were then fit as above. The fraction of D and H was then recalculated from the refined scattering length and the absorption recomputed. This procedure was repeated until no further changes occurred. Scattering amplitudes of  $0.94 \times 10^{-12}$  and  $0.96 \times 10^{-12}$  cm were assigned to N and Cl, respectively.

### B. Results

The 15 sets of data all gave about the same deuterium scattering length,  $b_D = (0.599 \pm 0.005) \times 10^{-12}$  cm. Allowing for systematic errors in the data this corresponds to a deuterium concentration of  $(93 \pm 2)\%$ , assuming scattering amplitudes of  $0.667 \times 10^{-12}$  and  $-0.374 \times 10^{-12}$  cm for D and H, respectively.

The final values of the Debye-Waller factors and the deuterium-positional parameters at each temperature are summarized in Table I. Observed and calculated intensities at 230 and 255 °K (below and above the transition) are listed in Table II, and are quite representative of the data as a whole. The crystallographic  $R$  factors ( $\sum |I_{\text{obs}} - I_{\text{calc}}| / \sum I_{\text{obs}}$ ) were around 3% on average. The values of the fitted order parameter as a function of temperature are given in Table III and Fig. 2. The matrix of correlation coefficients calculated for each refinement shows that the correlation between the order parameter and the other parameters is quite small ( $\leq 0.4$ ). In addition, the correlation matrices show that with the exception of the scale factor and extinction parameter, the parameters are well resolved.

In view of the fact that only a limited set of data could be collected at 1.25 Å, it was thought desirable to check these results by repeating the mea-

TABLE I. Results of the structure refinements for the Debye-Waller factors and deuterium positional parameter in ND<sub>4</sub>Cl as a function of temperature at atmospheric pressure. Scattering amplitudes taken as 0.94 and 0.96, both in units of  $10^{-12}$  cm, for N and Cl, respectively.  $B(N)$ ,  $B(Cl)$ , and  $B_{11}(D)$  are the isotropic factors for N, Cl, and D, respectively, and  $B_{12}(D)$  gives the anisotropy for deuterium.  $x(D)$  is the deuterium positional parameter. Standard errors are given in parentheses and refer to the least significant digits. The order-disorder transition falls between 248.85 and 248.86 °K. The deuterium-site scattering amplitude was also treated as a variable parameter and gave an average value of  $0.599 \pm 0.005$ , corresponding to  $(93 \pm 2)\%$  deuteration.

$T$ (°K)	$B(N)$ (Å <sup>2</sup> )	$B(Cl)$ (Å <sup>2</sup> )	$B_{11}(D)$ Å <sup>2</sup>	$B_{12}(D)$ (Å <sup>2</sup> )	$x(D)$
230	1.43(10)	1.35(10)	2.73(14)	-0.107(13)	0.1542(7)
242	1.54(9)	1.46(9)	2.89(14)	-0.103(11)	0.1540(7)
245	1.54(13)	1.51(12)	3.00(18)	-0.101(15)	0.1533(9)
247	1.68(12)	1.61(12)	3.05(18)	-0.128(16)	0.1540(9)
248	1.81(16)	1.73(16)	3.10(24)	-0.117(26)	0.1542(12)
248.5	1.61(12)	1.55(11)	2.99(15)	-0.107(18)	0.1537(9)
248.75	1.71(13)	1.61(12)	3.04(17)	-0.122(19)	0.1539(9)
248.8	1.62(13)	1.58(11)	3.03(15)	-0.119(21)	0.1537(9)
248.85	1.58(9)	1.53(8)	2.95(11)	-0.113(15)	0.1535(6)
$\longleftrightarrow T_c \longleftrightarrow$					
248.86	1.61(10)	1.55(9)	2.95(12)	-0.121(17)	0.1536(6)
248.815	1.57(11)	1.54(9)	2.91(12)	-0.120(18)	0.1538(7)
248.9	1.61(13)	1.60(11)	2.99(14)	-0.120(20)	0.1538(8)
249.0	1.64(13)	1.61(11)	3.02(13)	-0.120(19)	0.1536(7)
249.5	1.67(13)	1.69(12)	3.11(16)	-0.113(22)	0.1535(8)
255	1.72(12)	1.66(11)	3.15(14)	-0.131(18)	0.1534(6)

TABLE II. Observed and calculated neutron intensities from  $\text{ND}_4\text{Cl}$  in the ordered region at 230 °K and the disordered region at 255 °K, both at atmospheric pressure. Parameters as in Table I.

$hkl$	230 °K		255 °K	
	$I_{\text{obs}}$	$I_{\text{calc}}$	$I_{\text{obs}}$	$I_{\text{calc}}$
001	30.3	29.4	30.0	29.1
110	49.9	50.6	50.2	50.1
111	13.3	13.4	1.5	1.5
002	11.9	11.9	11.9	11.7
112	23.7	24.2	15.8	16.3
220	21.5	21.2	19.5	19.1
221	8.5	8.3	0.1	0.1
003	17.7	18.7	15.7	16.4
113	2.6	2.5	1.8	1.9
222	18.8	19.3	12.5	13.3
004	1.7	1.7	1.5	1.5
223	0.2	0.2	0.0	0.0
114	8.5	8.9	6.3	6.7
330	31.6	28.3	26.2	23.7
331	2.2	2.2	1.8	1.7
332	5.8	5.8	5.1	4.9
224	8.5	8.8	5.6	6.0

measurements with neutrons of shorter wavelength, which allows more reflections to be observed. This was done with a beam of 0.95-Å wavelength from a germanium (331) reflection. Thirty different peaks were measured at each of three temperatures and the data analyzed in exactly the same fashion as before. The values of the two sets of parameters, with the exception of the scale and extinction parameters which are expected to be different, lie within about two standard deviations or less, which can be considered quite satisfactory agreement. Representative figures are given in Table III.

### C. Conclusions

The results of the structure studies permit us to draw several important conclusions. There is a systematic increase in the Debye-Waller factors (Table I) as the temperature is raised which is quite normal, but *there is no significant change in the Debye-Waller factors in the immediate vicinity*

TABLE III. Structural parameters for  $\text{ND}_4\text{Cl}$  at 1 bar and 230 °K for neutron wavelengths of 0.95 and 1.25 Å.

	0.95 Å	1.25 Å
$\psi$	0.91(2)	0.86(3)
$x(\text{D})$	0.1540(4)	0.1542(7)
$b(\text{D})$	0.566(12)	0.599(19)
$B_{11}(\text{N})$	1.50(5)	1.43(10)
$B_{11}(\text{Cl})$	1.31(5)	1.35(10)
$B_{11}(\text{D})$	2.47(6)	2.73(15)
$B_{12}(\text{D})$	-0.11(1)	-0.11(1)
$R$ factor	0.06	0.04

of the order-disorder transition. This is consistent with the description of this system as Ising-like, in that it orders without appreciably changing the other properties of the system. Likewise, the deuterium positions are not sensitive to the transition, the atoms being roughly 1.03-Å distant from the nitrogen at all temperatures. These results are consistent with the Raman spectra for  $\text{NH}_4\text{Cl}$ ,<sup>6</sup> which are also only weakly sensitive to the transition. The magnitude of the librational motion of the tetrahedra as indicated by the Debye-Waller factors is small. Had this not been the case, the simple model described above, which does not include molecular rotations, would not be adequate to describe the data.

The second conclusion is that the order-parameter can be unambiguously determined from the structure measurements. Moreover, there is a considerable simplification. Of the 17 reflections studied with 1.25-Å neutrons, only the (221) and (111) reflections have substantial intensity resulting from the ordering. The latter also has considerable intensity in the disordered phase but the (221) has only a *very* small residual intensity above the transition. This almost complete disappearance is not due to any systematic absence resulting from symmetry. It results simply from the fortuitous cancellation of the nitrogen and chlorine contribution and the absence of any contribution from the deuterium above  $T_c$ . Furthermore, extinction effects and the change in the Debye-Waller factors are quite small over the range studied. In Table IV the order parameter  $\psi$  derived from the least-squares refinements is compared to the square root of the observed intensity of the (221) reflection as a function of temperature. It can be seen that within ex-

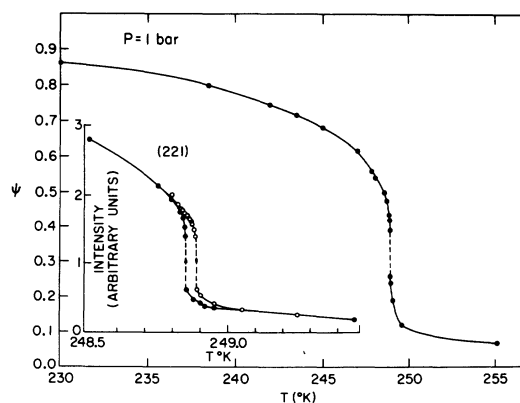


FIG. 2. Order parameter  $\psi$  as a function of temperature, at atmosphere pressure, showing a discontinuity at  $T_c \approx 248.86$  °K. The insert shows the intensity of the (221) reflection as a function of the increasing and decreasing temperature, and clearly reveals a hysteresis of  $\Delta T \approx 0.035$  °K.

TABLE IV. The value of the order parameter  $\psi$ , derived from the least-squares analysis of the structure data as a function of temperature at atmospheric pressure. Shown also is the square root of the observed (221) intensity normalized to  $\psi$  at  $T=230^\circ\text{K}$ . The standard errors are shown in parentheses and refer to the least significant digits. The data are corrected for a small residual Bragg peak at high temperature.

$T(^{\circ}\text{K})$	$\psi$	$(I_{221})^{1/2}$
230.0	0.861 (30)	0.861
242.0	0.745 (24)	0.740
245.0	0.681 (30)	0.684
247.0	0.614 (25)	0.611
248.0	0.541 (32)	0.550
248.50	0.498 (20)	0.495
248.75	0.430 (19)	0.435
248.8	0.419 (18)	0.418
248.85	0.389 (14)	0.386
← $T_c$ →		
248.865	0.259 (10)	0.254
248.875	0.254 (11)	0.252
248.9	0.238 (12)	0.236
249.0	0.192 (15)	0.193
249.5	0.118 (25)	0.125
255.0	0.067 (10)	0.068

perimental accuracy, the order parameter is proportional to the square root of the (221) intensity, and can therefore be measured as a function of temperature or pressure simply by following the latter. This is an important practical feature in the phase studies described in Sec. IV. In addition, critical scattering can be measured much more accurately if the Bragg peak is small or absent.

It can be seen from Table IV and Fig. 2 that a nonzero value for  $\psi$  is obtained above the phase transition at  $248.86^\circ\text{K}$ . This is due to the inclusion of the critical scattering in the total fitted intensity. Since collimation was absent between sample and detector, the resolution did not permit even a qualitative separation of the Bragg and critical contributions. However, even in these data there is some evidence that above  $T_c$  the linewidths observed are greater than those observed in the ordered phase, as would be expected. Quite surprising, however, is the large intensity of the critical scattering and its persistence well above the phase transition.

#### D. Order of the transition

While it is well known that the atmospheric pressure phase transition in  $\text{NH}_4\text{Cl}$  at  $T \approx 242^\circ\text{K}$  is first order<sup>10,12</sup> there has been considerable uncertainty about the transition in  $\text{ND}_4\text{Cl}$ .<sup>2,3</sup> The results of our structure work show a distinctly discontinuous order parameter. Further confirmation of the first-order nature of the transition was obtained by observing the intensity of the (221) reflection<sup>29</sup> as a

function of temperature in the vicinity of the transition (Fig. 2 insert). At each temperature the reflection was scanned and the intensity integrated over the five highest points. The resulting curve clearly shows hysteresis with a  $\Delta T_c$  of about  $0.035^\circ\text{K}$  (compared to  $\Delta T_c$  of about  $0.3^\circ\text{K}$  for  $\text{NH}_4\text{Cl}$ ) which classifies the transition as first-order. The magnitude of the intensity discontinuity was the same for both heating and cooling. To within the sensitivity of the controller,  $\sim 0.001^\circ\text{K}$ , no rounding of this discontinuity could be observed. The transition temperatures were reproducible to within about  $0.003^\circ\text{K}$  upon recycling.

It is somewhat surprising that no rounding of  $T_c$  could be seen, especially in view of the significant fraction of hydrogen in this deuterated material. This suggests that the interactions in  $\text{NH}_4\text{Cl}$  and  $\text{ND}_4\text{Cl}$  are very nearly equal in strength, their differences being due only to the difference in lattice constants for the two materials. It would be interesting to confirm this hypothesis by studying other members of the series with different ratios of H and D.

## IV. PRESSURE MEASUREMENTS

### A. Experimental

For these measurements, another rather larger sample, roughly  $3 \times 3 \times 4$  mm, was mounted with a [110] axis vertical in the aluminum high-pressure vessel illustrated in Fig. 3, which had a cylindrical sample chamber 5 mm in diameter. The crystal was clamped in a small aluminum frame which was held firmly in position by a spring. The vessel was pressurized with helium gas, and pressures of up to 6 kbar could be attained.<sup>30</sup> Up to 2.5 kbar the pressure was read directly from a Bourdon gauge with a precision of 1.5 bar. For higher pressures a manganin-resistance sensor was employed together with a Wheatstone bridge coupled to an external dc null detector. The sensor was calibrated against the Bourdon gauge below 2.5 kbar, and pressures

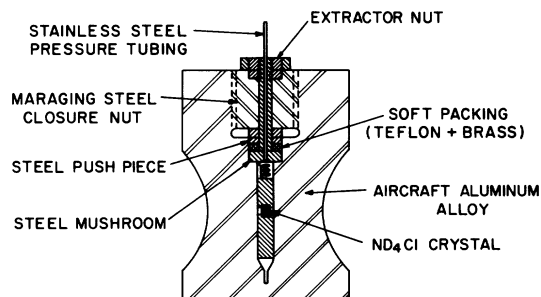


FIG. 3. Aluminum pressure vessel used for measurements up to 6 kbar. The cell is pressurized with helium gas and the pressure monitored with a Bourdon gauge and manganin resistance sensor.

above this were determined by linear extrapolation. The sensitivity was about 1 bar at all pressures. Absolute pressures were known with considerably less accuracy, however, owing to zero errors in the Bourdon gauge. An estimate is  $\pm 10$  bar at low pressures and  $\pm 40$  bar at high pressures.

An additional temperature sensor was embedded in the pressure vessel, which was then mounted in a temperature controlled Dewar. The sample temperature was regulated by a sensor mounted in the heat sink of the Dewar, but measured with the sensor in the pressure vessel. Relative temperatures could be controlled and measured to within  $0.005^\circ\text{K}$ . Absolute errors are typically within  $0.1^\circ\text{K}$ . The time required for temperature equilibrium after the regulating sensor had reached the control point was about 30 min. In contrast, pressure changes could be achieved nearly instantaneously and from this point of view pressure was the preferred variable. However, temperature scans were made in a number of cases despite the long time constants.

#### B. Measurements of the Bragg intensity

In order to evaluate the order-parameter  $\psi$  and obtain an accurate value for the critical exponent  $\beta$ , it is necessary to subtract the critical scattering from the total observed intensity, in the vicinity of the phase line. This is usually done in one of two ways: either by estimating the Lorentzian contribution from an examination of the line shape of the scattered intensity, or by making some symmetry assumption relating the critical scattering below  $T_c$  to that observed above (e.g., scaling the intensity by a factor of  $\frac{1}{2}$ ). Neither method is entirely satisfactory and we have attempted to make these corrections more quantitative by decomposing the observed line shapes into Bragg and critical scattering contributions.

All data were taken with an incident incoming neutron beam of wavelength  $1.18 \text{ \AA}$  from a pyrolytic graphite monochromator in the (004) position. Coupled ( $\theta$ - $2\theta$ ) scans of the (221) reflection were made at detector intervals of  $0.06^\circ$  through an angle of  $2\theta_B \pm 3^\circ$ . In addition to the collimation previously used, a  $20'$  collimator was used in front of the detector. The data were fitted by means of a nonlinear least-squares program to the sum of a Gaussian for the Bragg contribution, a Lorentzian of Ornstein-Zernike form folded with the resolution function to describe the critical scattering, and a constant background. The width of the Gaussian contribution was determined by fitting the Bragg data far from the transition, where the critical scattering can be assumed to be zero. Within error limits, this width was temperature and pressure independent and very nearly equal to the calculated resolution width. The background was ob-

served at  $2\theta_B - 5^\circ$  and found to be constant in the range of interest. The variable parameters in the refinement were therefore the amplitudes of the Gaussian and Lorentzian peaks and the width of the latter.

While this kind of approach has previously been used to analyze critical scattering,<sup>31</sup> the method generally employed has been to evaluate directly the full three-dimensional folding integral. This is a long, slow process and a typical refinement with 40 data points in the scan would take up to 1 h of fast computer time (CDC - 6600) with only about 1% accuracy in the evaluation of the integral. Frequently, too, the refinement may not converge or converges to a local minimum if starting parameters are not well chosen. The procedure is, therefore, expensive and tedious. It has recently been pointed out,<sup>32</sup> however, that a Laplace transformation exists which permits the exact evaluation of part of the integration and reduces the numerical work to a one-dimensional integral. The evaluation of this integral was further speeded by the use of Gaussian quadratures. With these techniques, refinement of a scan containing 64 data points, to at worst 0.1% error in the value of the integral (the error is  $\kappa$  dependent), was typically completed in 40 sec on the same computer. The method therefore becomes practical as a general tool and has been employed extensively in the present study. It gives very satisfactory and quite consistent results for the Bragg contribution, even when the critical scattering contribution is substantial (Figs. 4 and 5) and we were able, in most cases, to obtain values for  $\psi$  one-half decade or more toward the critical point than would otherwise have been possible. Furthermore, the values obtained for the inverse correlation length  $\kappa'$  were qualitatively

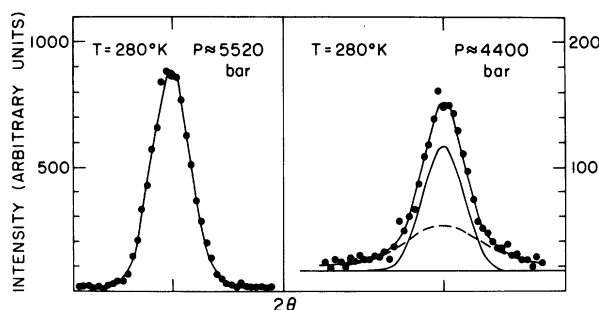


FIG. 4. Typical raw intensity data at  $280^\circ\text{K}$ . At 5520 bar, there is only Bragg scattering with approximately the calculated resolution linewidth. At 4400 bar the peak is noticeably broader and can be decomposed into a Bragg component with the same half-width as at 5520 bar (solid line), together with a Lorentzian folded with the resolution function (broken line). Note the change of scale; the background is in fact constant.

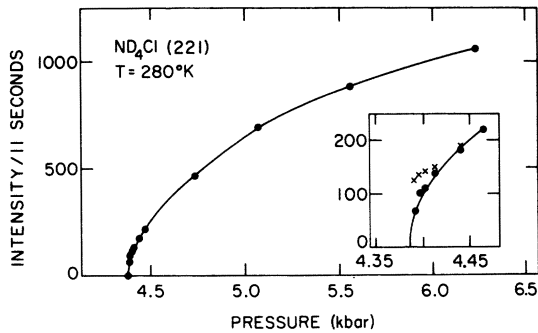


FIG. 5. Variation of the (221) intensity at 280°K as a function of pressure, corrected for the critical scattering. The insert shows an expanded scale the region close to  $T_c$ , with the uncorrected peak intensities denoted by crosses and the corrected values by filled circles.

reasonable;  $\kappa'$  decreased systematically as the critical point was approached. The uncertainty in  $\kappa'$  was considerable, however, due to a fairly large correlation between  $\kappa'$  and the Lorentzian amplitude (particularly for large values of  $\kappa'$ ). For  $\kappa' < 0.01 \text{ \AA}^{-1}$ , this analyzing procedure broke down as the resolution of the spectrometer was insufficient to enable the Bragg and critical scattering to be distinguished. This was not a serious limitation on the determination of  $\beta$  since measurements of  $\psi$  covered between two and three decades over a range below 0.1 in reduced units; however, the evaluation of  $\nu'$  was not possible.

The results of the analysis give the peak intensity for the Bragg component, but since the entire peak is used in the evaluation, the statistical errors are equivalent to those expected from a determination of the integrated intensity. It should be noted that when simpler expressions were chosen to approximate the critical scattering, such as a simple Lorentzian, or a Lorentzian folded with a one-dimensional Gaussian, the results for both  $\kappa'$  and  $\psi$  were significantly less satisfactory.

### C. Determination of TCP

Preliminary studies of the pressure dependence of  $\psi$  in  $\text{ND}_4\text{Cl}$  indicated that the transition became continuous between 50 and 200 bar, but it is quite difficult to observe a small discontinuity in  $\psi$  when significant critical scattering is present, and we were unable to localize the TCP better than this from this type of measurement. Furthermore, the hysteresis observed at atmospheric pressure becomes smaller and hence more difficult to measure when the pressure is raised and is therefore not a very satisfactory probe for this purpose. The critical scattering, on the other hand, should be a sensitive indicator of the TCP, since the correlation length and susceptibility diverge along the second-order phase line and at the TCP, but not along the

first-order line. Along the phase line, therefore, the critical scattering should be discontinuous at the TCP.

Initially, the critical scattering was studied as a function of pressure at scattering angles sufficiently far from  $2\theta_B$  for there to be no contribution from the wings of the Bragg peak. These scans were useful for defining the phase line (Fig. 6) since the critical scattering peaks dramatically near  $T_c$ , but no significant change relating to the order of the transition was observed. This is not surprising since the divergence in the susceptibility produces a sharp intense line, and little scattering at large values of  $\Delta(2\theta_B)$  is to be expected.

In principle, measurements of the peak intensity of the critical scattering taken exactly along the phase line would certainly reveal the TCP, but with both the pressure and temperature as variables, it is impossible in practice to make such a scan without wandering into and out of the ordered region. What was actually done, however, is closely related to this. The peak intensity of the critical scattering was measured in the disordered region along lines roughly parallel to the phase line (Fig. 7). The earlier attempts to localize the TCP had defined the latter well enough for scans to be made without crossing into the ordered region, but since

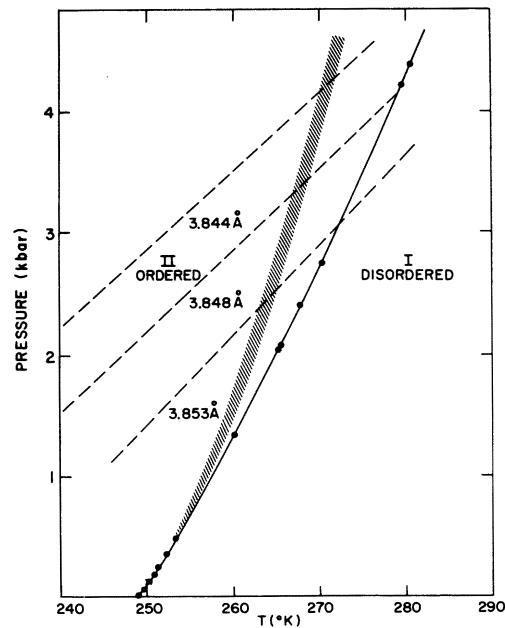


FIG. 6.  $P$ - $T$  phase diagram for  $\text{ND}_4\text{Cl}$  in the order-disorder region. The broken lines indicate contours of constant lattice parameter, and the shaded area represents the cross-over region from second-order to tricritical behavior. Each filled circle indicates a transition point determined either by a constant pressure or a constant temperature scan.

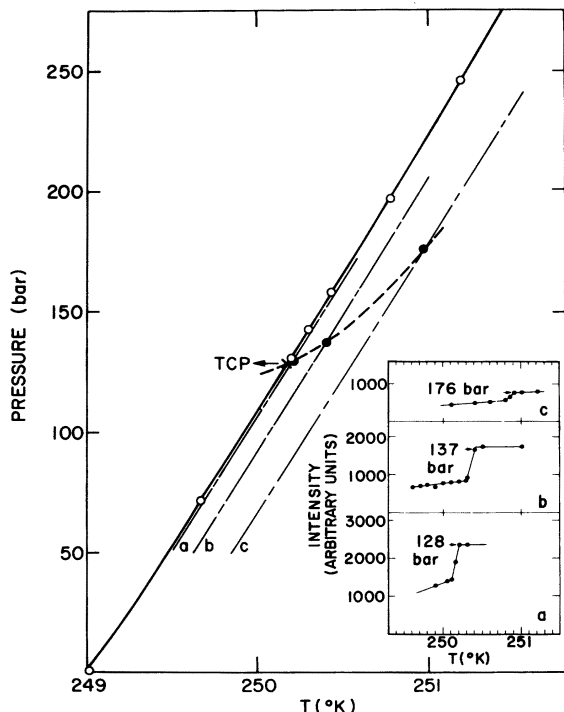


FIG. 7. Phase diagram for  $\text{ND}_4\text{Cl}$  in the vicinity of the tricritical point. The closed circles correspond to the midpoint of the sharp increase in the peak intensity of the critical scattering observed for scans along the broken lines *a*, *b*, and *c* in the disorder region, as shown in the insert. Note that the magnitude of this increase becomes smaller and moves to higher pressures for scans further away from the phase line.

both pressure and temperature had to be varied, these measurements were quite tedious and time consuming. It was expected that the change in critical behavior at the TCP would be reflected in an

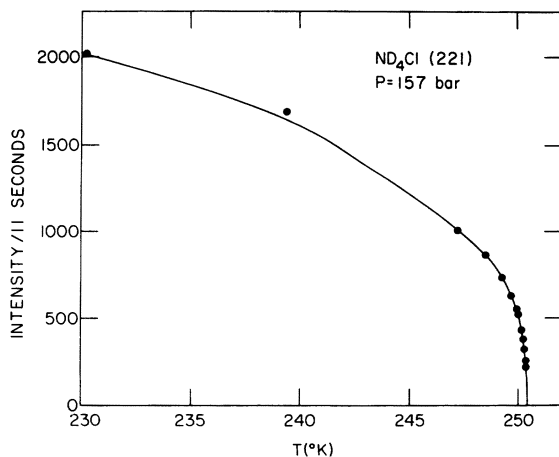


FIG. 8. Variation of the (221) intensity as a function of temperature at 157 bar.

appreciable change in intensity along these lines, but the almost steplike behavior actually observed was rather surprising (Fig. 7 insert). The magnitude of the step decreases, but it remains quite distinct further away from the phase line. It was verified, however, from measurements made along the rise that it is continuous. We believe that the extrapolation to the phase line of the midpoint of these rises (or endpoints) gives an accurate determination of the TCP. This extrapolation yields values of  $(128 \pm 10)$  bar and  $(250.2 \pm 0.1)$  °K.

These measurements suggest rather unusual geometry for the susceptibility contours in the neighborhood of the TCP; the steplike behavior indicates a "pseudotransition" line extending from the TCP. Such a pseudotransition line can be generated from mean-field models of tricritical behavior although detailed calculations do not exist for  $\text{ND}_4\text{Cl}$ .

#### D. Results

A series of measurements of the order parameter as a function of temperature at constant pressure and pressure at constant temperature were made through various points along the phase line, including one scan of each type in the neighborhood of the TCP. The first of these, a temperature scan at 157 bar, which has been corrected for critical scattering as previously discussed, is shown in Fig. 8. The intensity remains quite high as the temperature is raised, and then drops precipitously close to the transition, which is characteristic of a low exponent. These data can be fit very well to a simple power law  $I = A(T_c - T)^{2\beta}$  from 230 to 250.39 °K, with the transition temperature included as a fitting parameter (Fig. 9). We find:  $2\beta = 0.36 \pm 0.01$  and  $T_c = (250.43 \pm 0.01)$  °K. The absolute value of  $\psi$  was not known sufficiently well to permit an accurate evaluation of the amplitude factor. Within the error limits, the fitted transition temperature agrees with the value determined independently by observing the intensity of the critical scattering beyond the wings of the Bragg peak.

Another scan near the TCP was made as a func-

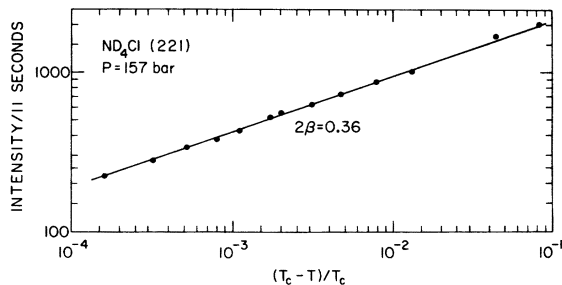


FIG. 9. Logarithmic plot of the (221) intensity as a function of temperature at 157 bar.



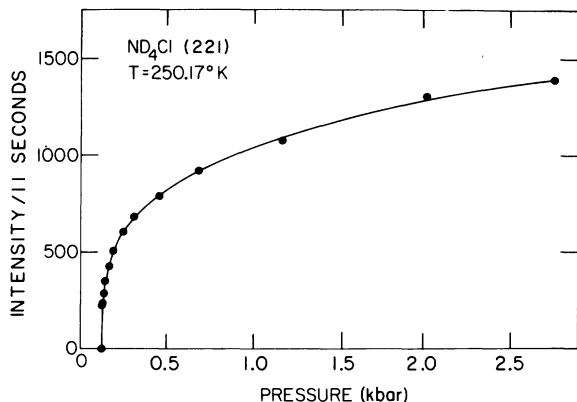


FIG. 10. Variation of the (221) intensity as a function of pressure at 250.17 °K.

tion of pressure at 250.17 °K (Fig. 10). The same general shape is seen as in Fig. 8, and the data again can be fit well to a simple power law,  $I = B(P - P_c)^{2\beta}$  (Fig. 11) with  $2\beta = 0.28 \pm 0.01$  and  $P_c = (127 \pm 1)$  bar. The latter figure is very close to the TCP values discussed in Sec. IVC and is in good agreement with that deduced from the critical scattering.

Both scans near the TCP obey the simple power law over a reduced range  $g < 0.1$ , where  $g$  is defined as  $(T_c - T)/T_c$  or  $[(P - P_c)/T_c](dT_c/dP)$  for constant pressure and constant temperature scans, respectively.<sup>33</sup> The difference in the exponents for these two measurements is significantly outside their error limits, and cannot be attributed to the small difference in  $T_c$ . Since almost three decades in terms of reduced units were measured in both cases, and since critical scattering corrections were quite small, it is unlikely that the difference in exponents is due to small systematic errors close to  $T_c$  in one or both sets of measurements.

Two similar runs were made in the vicinity of  $T_c = 280$  °K, which was the highest temperature at which the required upper pressure limit could be safely attained. The constant temperature data shown in Fig. 5 display a pressure dependence dramatically different from that seen at 250 °K (Fig.

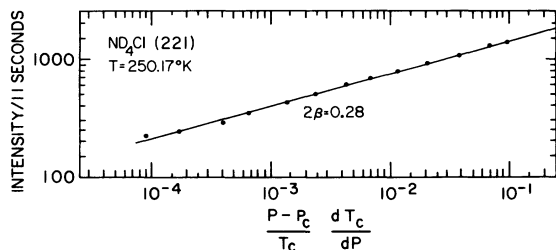


FIG. 11. Logarithmic plot of the (221) intensity as a function of pressure at 250.17 °K.

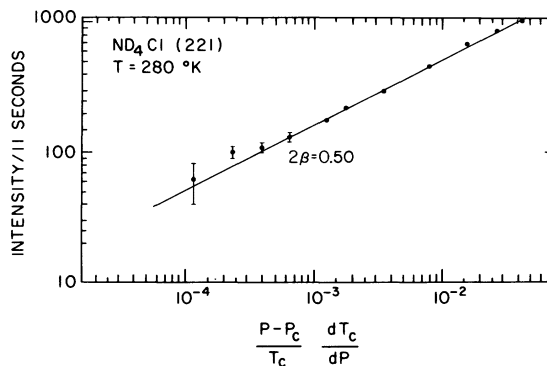


FIG. 12. Logarithmic plot of the (221) intensity as a function of pressure at 280.0 °K.

10). Far from the transition the decrease in intensity with decreasing pressure is more rapid, but near the transition less precipitous than at 250 °K. These data were again fitted to a simple power law with  $2\beta = 0.50 \pm 0.04$  (Fig. 12). The error bars reflect both the smaller intensities close to  $T_c$  and also the larger contributions from the critical scattering to the data, which causes greater uncertainties in the least-squares analysis. However, better resolution and a larger sample will surely permit a reduction in these error bars in the future.

The constant-pressure data at 4140 bar reproduced in Fig. 13 show a new feature, in that a single power law no longer appears to hold over the whole range to  $g \sim 0.1$  (Fig. 14). For  $g \leq 0.02$ ,  $2\beta = 0.61 \pm 0.04$ , in good agreement with the three-dimensional Ising value for a second-order transition. However, for  $0.1 \geq g > 0.02$ , there is a definite change in slope, indicative of a lower exponent. Since a power law is valid to  $g = 0.1$  in the other cases described so far, there is no reason to believe that its breakdown here is due to saturation effects, particularly since the intensity at  $g = 0.1$  is less than the corresponding intensity for the constant pressure scan at 157 bar. It is be-

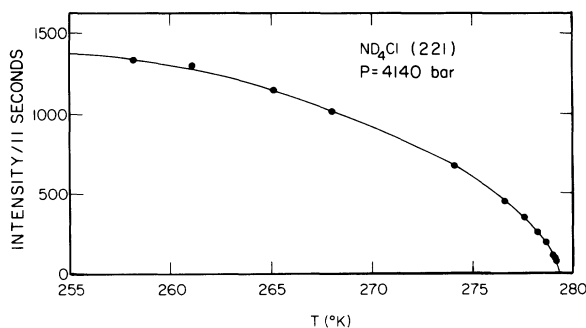


FIG. 13. Variation of the (221) intensity as a function of pressure at 4140 bar.

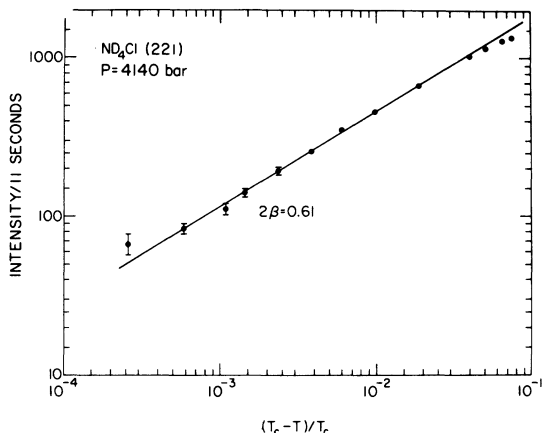


FIG. 14. Logarithmic plot of the (221) intensity as a function of temperature at 4140 bar. Note the change of slope believed to be indicative of cross-over behavior between second-order and tricritical regions.

lieved that the change in slope indicates "cross-over" behavior from the second-order region close to the phase line, to the tricritical region further away. Furthermore, if current models are correct, the width of the second-order region so defined should shrink as the tricritical point is approached, and this is exactly what is observed. However, if the second-order region is too large, the tricritical region is not seen, as is the case for the constant-temperature scan at 280 °K. Likewise, if it is too small, the regions are not sufficiently distinct for two exponents to be defined and only some average value is measured. For example, in the constant temperature scan at 260 °K, one sees only an intermediate value;  $2\beta = 0.38$  compared to 0.28 at the TCP and 0.50 at 280 °K. However, at 265 °K one sees an inner exponent quite close to the 280 °K value (Fig. 15). Enough observations of the cross-over behavior were made to give a qualitative indication of the extent of the tricritical and second-order regions of

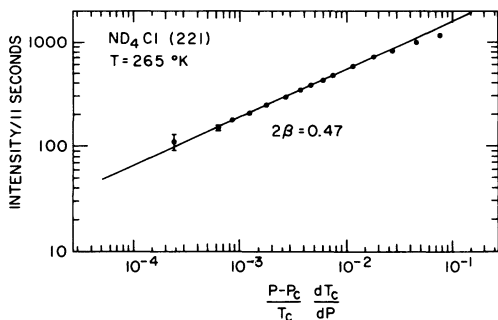


FIG. 15. Logarithmic plot of the (221) intensity as a function of pressure at 265 °K. A change in slope similar to that seen at 4140 bar is also seen in this case.

the phase diagram (Fig. 6). Scans as a function of pressure and temperature were made to a number of intermediate transition points between 250 and 280 °K, and these indicate that the  $2\beta$  values observed at 280 °K are close to the asymptotic limit, so that close to the phase line at 280 °K one sees truly second-order behavior.

Although the absolute value of the amplitude factor was not determined for any scan, the ratio of amplitudes for different scans at fixed pressures, where the proper reduced quantity is unambiguously defined, could easily be determined. In particular, the amplitude  $A$  ( $\psi/\psi_0 = Ag^\beta$ ) at 4140 bar is a factor of  $1.25 \pm 0.02$  greater than the amplitude at 157 bar close to the TCP.

Scans were also made below the TCP, in the first-order region. Data were collected at atmospheric pressure (see Sec. III A) and at a constant temperature of 249.68 °K, 0.5 °K below the TCP. Both sets of data could be fitted to a power law very satisfactorily, but the fitted values of the transition temperature and pressure were, respectively, higher and lower than those actually observed, as might be expected. The corresponding exponents are  $2\beta = 0.27 \pm 0.01$  for  $T = 249.68$  °K (Fig. 16) and  $2\beta = 0.31 \pm 0.02$  for  $P = 1$  bar (Fig. 17). While the first is in good agreement with the TCP results, the difference between the  $P = 1$  bar and the  $P = 157$  bar data is significant and demonstrates that great care must be taken in the interpretation of any exponents calculated when the transition is first order.

#### E. Studies of critical scattering

The interpretation of the data in the ordered region required decomposition of the scattering into Bragg and critical components and in this process some information was obtained about the short-range correlations in the ordered phase. The critical scattering has also been studied in the high-temperature disordered phase. Although the accuracy of most of the data is not high, there are several remarks that can be made about the gen-

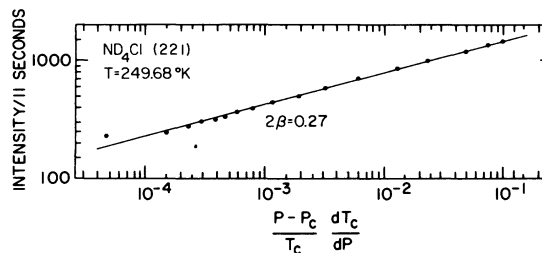


FIG. 16. Logarithmic plot of the (221) intensity as a function of pressure at 249.68 °K. This is in the first-order region and the fitted  $P_c$  is lower than that actually observed.

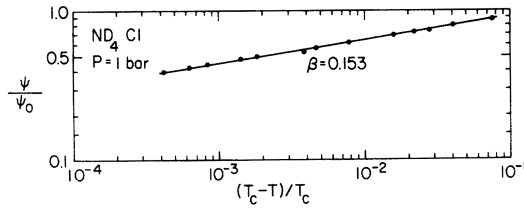


FIG. 17. Logarithmic plot of the order-parameter calculated from the structure data at atmospheric pressure. This is in the first-order region and the fitted  $T_c$  is about 0.1 °K higher than that actually observed.

eral nature of the critical scattering.

In the ordered phase the critical scattering near the TCP is quite small compared to that at 280 °K. The corrections for critical scattering become negligible beyond  $g = 0.002$  at 157 bar, but not until  $g = 0.006$  at 4140 bar. At present, it is not possible to determine whether this difference occurs mainly in the exponent or the amplitude for critical scattering, though the latter is more probable. This behavior can be understood in the following qualitative manner. Near the TCP where the exponent  $\beta$  is quite small, the system orders very rapidly as the temperature is lowered, and for small values of  $g$  the order parameter is much larger than in the second-order region. As a result of this rapid long-range ordering, the system is less free to fluctuate and hence the critical scattering is small.

In the disordered phase, on the other hand, the critical scattering at the TCP is very much larger than in the second-order region, perhaps by a factor of about 3. Furthermore, at 130 bar critical scattering is readily observed more than 20 °K above  $T_c$ , and is still weakly visible 30 °K above.

The data taken at 130 bar as a function of temperature have been carefully analyzed by the same methods used for the ordered region. The very small residual Bragg contribution (mentioned in Sec. III C) and the background were determined at 280 and 290 °K and held fixed in the refinements at lower temperatures.

The wave-vector-dependent susceptibility, which has the form<sup>34</sup>

$$\frac{\chi(\vec{q})}{\chi(0)} = \frac{(1/r_1)^{2-\eta}(\kappa^2 + \phi^2 q^2)^{\eta/2}}{\kappa^2 + \psi q^2}, \quad (3)$$

where  $\kappa$  is the inverse correlation length,  $q$  is the offset of the spectrometer from the center of the response function, and  $\eta$  is the parameter describing the deviation from the Ornstein-Zernike form, was initially analyzed using the Fisher-Burford<sup>34</sup> first approximant

$$\frac{\chi(\vec{q})}{\chi(0)} = \frac{A}{(\kappa^2 + q^2)^{1-\eta/2}}, \quad (4)$$

where  $A$ ,  $\kappa$ , and  $\eta$  are all parameters to be determined. Unfortunately, the resolution was not sufficiently good for the parameters to be refined simultaneously, and  $\eta$  was held fixed at various values. The best results were obtained for  $\eta = 0.0 \pm 0.05$ . It was subsequently pointed out,<sup>35</sup> that the form in Eq. (4) gives, in most cases, less satisfactory results than the Fisher-Burford zeroth approximant (which is the Ornstein-Zernike form), in agreement with the above value of  $\eta$ .

A better approximation to the form of the critical scattering is likely to be<sup>35</sup>

$$\chi(q)/\chi(0) = A\kappa^\eta/(\kappa^2 + q^2) \quad (5)$$

for  $T > T_c$  and  $q < \kappa/\Phi$ , which will show a nonzero  $\eta$  only if  $A$  is held constant. In the limit  $T \approx T_c$  (i. e.,  $\kappa \ll \Phi q$ ) the form

$$\chi(q)/\chi(0) = A\phi^\eta/q^{2-\eta} \quad (6)$$

should be valid, enabling one to evaluate  $\eta$ . Unfortunately, because of the relatively poor resolution, the data were not of sufficient quality to permit this to be done.

In the region where the analysis could be performed satisfactorily,  $A$  was nearly constant and  $\kappa$  could be fit to a power law  $(T - T_c)^\nu$  with  $\nu = 0.52 \pm 0.08$ . The resulting value for  $\gamma$  is  $1.05 \pm 0.20$ . The error bars are so large that this value can only be considered a preliminary one.

Although these measurements were intended only as a preliminary survey of the critical scattering, it is clear from the results that with a suitably large crystal one should be able to determine all of the susceptibility exponents,  $\gamma$ ,  $\gamma'$ ,  $\nu$ ,  $\nu'$ ,  $\eta$  and  $\eta'$ , both near the TCP and in the second-order region with reasonable accuracy. Furthermore, recent diffuse-x-ray studies of NH<sub>4</sub>Cl near the transition have shown critical scattering characteristic of the tetragonal NH<sub>4</sub>Br phase<sup>36</sup> (see Sec. V), and it should be possible from neutron measurements to determine the susceptibility exponents corresponding to the nonordering density.

## V. DISCUSSION AND CONCLUSIONS

In order to understand the results for ND<sub>4</sub>Cl, it is necessary to introduce a plausible phase diagram for the system. We can then discuss the apparent violation of the smoothness postulate and make a short comparison of our results with current theories.

Tricritical points arise in systems which can have "competing" order parameters. In the case of the ammonium halides, there is an octupole-octupole nearest-neighbor coupling which favors the parallel ordering of tetrahedra observed in ND<sub>4</sub>Cl,

and in  $\text{NH}_4\text{Br}$  and  $\text{NH}_4\text{I}$  at sufficiently high pressures, and an octupole-dipole-octupole "super-exchange"<sup>37</sup> (via the intervening halide ion) which predominantly favors the antiparallel ordering observed in  $\text{NH}_4\text{Br}$  and  $\text{NH}_4\text{I}$  at atmospheric pressure.<sup>38</sup> Each type of ordering can be characterized by an order parameter and a conjugate ordering field, though these fields are inaccessible to experiment. Denoting the parallel and antiparallel ordering fields by  $\zeta$  and  $H$ , respectively, we obtain (based on a mean-field calculation) the phase diagram for  $\text{ND}_4\text{Cl}$  shown in Fig. 18. The second-order line in the  $H$ - $T$  plane bifurcates at the TCP and continues as boundaries of two first-order coexistence surfaces (wings) that extend out of the  $H$ - $T$  plane. Similar phase diagrams can be obtained for metamagnets (such as  $\text{FeCl}_2$  and DAG) with the role of antiparallel and parallel ordering field reversed.<sup>14,39</sup>

It is possible that the "pseudospin"-lattice coupling and the octupole-octupole exchange alone are sufficient to produce a tricritical point (compressible-Ising model) as certain models suggest, but in the present case the presence of critical scattering at the zone boundary indicates that the antiparallel exchange plays a fundamental role.

If we combine the behavior of  $\text{ND}_4\text{Cl}$  in the  $H$ - $T$  plane with the pressure dependence which was observed experimentally, we obtain the  $H$ - $T$ - $P$  phase diagram shown in Fig. 19. At pressure  $P_1$  a cut parallel to the  $H$ - $T$  plane will reproduce the diagram shown in Fig. 18. At pressure  $P_2$ , however, the TCP will have moved to  $H=0$  and for  $0 \leq P \leq P_2$  no second-order line will be visible in any cut parallel to  $H$ - $T$ . It is possible that at some pressure  $P_4$  the TCP will "disappear" at  $T=0$  and hence we anticipate that in the  $H$ - $T$ - $P$  space there will be a

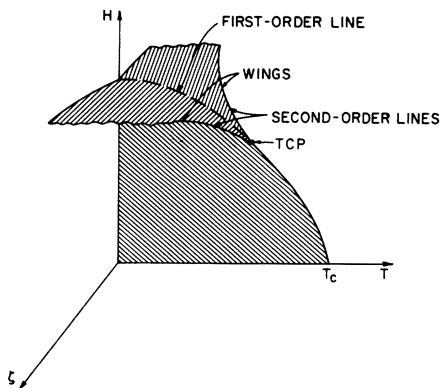


FIG. 18. A plausible phase diagram for  $\text{ND}_4\text{Cl}$ .  $H$  is a field conjugate to the antiferromagnetic ordering, while  $\zeta$  is conjugate to the ferromagnetic ordering. The second-order line bifurcates at the TCP and continues as the boundary of the wings.

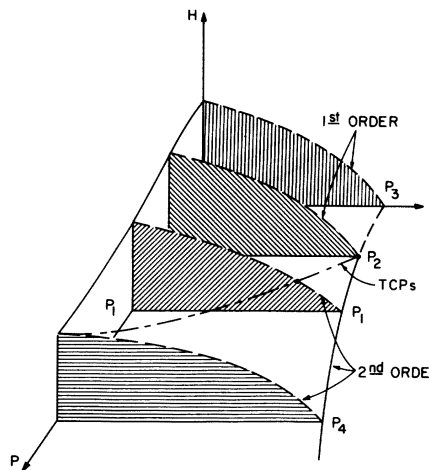


FIG. 19. A plausible phase diagram for  $\text{ND}_4\text{Cl}$  in  $H$ - $T$ - $P$  space. There is a line of TCP's beginning at  $P_2$  and  $H=0$ , and terminating at  $P_4$  and  $T=0$ , which divides the space into surfaces of first- and second-order phase transitions. The section at  $P_1$  contains the features of the  $H$ - $T$  plane in Fig. 18.

line of TCP's between  $T=0$ ,  $P=P_4$  and  $H=0$ ,  $P=P_2$  separating surfaces of first- and second-order transitions.<sup>40</sup> In accord with the ideas of smoothness,<sup>41</sup> we expect that the asymptotic critical behavior of  $\text{ND}_4\text{Cl}$  can be characterized by a single set of second-order exponents and by a single set of tricritical exponents. Thus everywhere along the line of TCP's one expects to measure the same set of critical exponents. This leads to the interesting consequence that the basic description of tricritical behavior can be obtained from  $P$ - $T$  measurements of  $H=0$ ; that is, in the absence of the "nonordering density." Therefore, no "demagnetizing" corrections are necessary, corrections which are quite important for metamagnets.

Let us consider further, now, the ideas of smoothness in the  $P$ - $T$  plane. One result of our experiment is that the measured critical exponent  $\beta$  depends upon the direction along which one approaches the phase line.<sup>42</sup> In addition, the  $\beta$  characterizing a particular direction appears to change in a continuous fashion as one moves along the phase line. Smoothness, of course, requires that the value of  $\beta$  be the same for all "nonasymptotically parallel" approaches to the critical line.

The smoothness postulate<sup>41</sup> deals with an asymptotic exponent which experimentally can be identified as the limit of an "effective" exponent obtained by fitting  $\ln\psi$  vs  $\ln|g|$  over a certain number of decades as the distance from the critical line shrinks to zero. The continuous variation of  $\beta$  is then easily understood as resulting from fitting data which extend beyond this asymptotic range. This range shrinks as one approaches the TCP in

accord with current theory due to the cross-over effects mentioned previously.

The observed difference in exponents for different directions of approach to the same point may be due to similar effects. According to the theory of Griffiths and Wheeler, critical behavior along a second-order critical line can be described by two independent thermodynamic fields, one of which must be chosen in some sense parallel to the phase line. These two fields define directions of approach to the phase line each of which is characterized by a different exponent. In scaling theory, one measures in the asymptotic limit the exponent characteristic of the nonparallel direction for all paths except the asymptotically parallel path. However, if one follows a path that is close to the parallel path, the exponent will not reach its limiting value at measurable distances. We believe this to be the case for constant temperature measurements. This direction must become closer to the parallel direction as pressure is raised and the lattice becomes less compressible. Hence, exponents measured in this direction may deviate from the expected results. The temperature axis, on the other hand, should be more pure, and the observation of an Ising-like  $\beta$  at high pressures tends to bear this out. One may be able to verify these speculations by the measurement of the other critical exponents along this line since simple scaling should hold in the pure direction and appear to break down in the nearly parallel direction.

The value measured for the tricritical  $\beta$  ( $\sim 0.18$ ) is in reasonable accord with present models. One of these, largely due to Riedel and Wegner,<sup>15</sup> predicts that the TCP,  $\psi \propto (g \ln g)^{1/4}$ , i. e.,  $\beta = \frac{1}{4}$ . However, the logarithmic correction results in a  $\beta_{\text{eff}} \approx 0.19$  if one fits the function  $(g \ln g)^{1/4}$  to a power

law  $g^{\beta_{\text{eff}}}$  over the range  $10^{-1}$ – $10^{-4}$ . Another model, based on an extension of the Schofield equation of state<sup>43</sup> to the TCP<sup>18</sup> gives a value for  $\beta$  which depends weakly on the geometry of the phase lines but is approximately 0.17.

Because of the previously mentioned absence of demagnetizing effects, ND<sub>4</sub>Cl is in many respects a nearly ideal system for studying tricritical effects. The picture presently available is a very consistent one; the values of  $\beta_i$  are in general agreement with theory, as is the cross-over behavior. A wealth of further information should be available when a more thorough study of the critical scattering is completed. Coupled with a thermodynamic measurement of  $\alpha$ , the neutron measurements of  $\beta$  reported here, the susceptibility exponents  $\gamma$ ,  $\nu$ , and  $\eta$ , and the related low-temperature and nonordering quantities should provide a test of scaling at the TCP.

It would also be of great interest to study the discontinuity in  $\psi$  as a function of the distance from the TCP, in the first-order region. Unfortunately, in ND<sub>4</sub>Cl this region is quite small and a careful survey would be quite difficult. However, in N(H<sub>0.5</sub>D<sub>0.5</sub>)<sub>4</sub>Cl the coherent scattering may be sufficient to permit accurate measurement and the first-order region may be large enough to indicate whether the scaling predictions<sup>33</sup> linking this region to the TCP have any validity.

#### ACKNOWLEDGMENTS

The authors would like to thank J. Skalyo, Jr. for his assistance with the fitting programs, and W. Cralley for performing many of the computer calculations. We would also like to acknowledge several useful discussions with R. J. Birgeneau, D. Hunter, M. Blume, and G. Shirane.

\*Work performed under the auspices of the U. S. Atomic Energy Commission.

†Present address: Institut Laue-Langevin, Grenoble, France.

‡Present address: I. F. F. -K. F. A. Jülich, Germany.

<sup>1</sup>F. Simon, Ann. Phys. **68**, 241 (1922). P. Schwartz, Phys. Rev. **34**, 920 (1971).

<sup>2</sup>P. Nissila and J. Poyhonen, Phys. Lett. A **33**, 345 (1970).

<sup>3</sup>A. A. Boiko, Sov. Phys. Crystallogr. **14**, 539 (1970).

<sup>4</sup>G. E. Fredericks, Phys. Rev. B **4**, 911 (1971).

<sup>5</sup>C. W. Garland and C. F. Yarnall, J. Chem. Phys. **44**, 3678 (1966).

<sup>6</sup>C. H. Wang and R. B. Wright, J. Chem. Phys. **56**, 2124 (1972).

<sup>7</sup>M. Tokunaga and N. Koyano, J. Phys. Soc. Jap. **24**, 1407 (1968).

<sup>8</sup>S. Ueda and J. Itoh, J. Phys. Soc. Jap. **22**, 927 (1967).

<sup>9</sup>N. J. Trappeniers and Th. J. Van der Molen, Physica **32**, 1161 (1966).

<sup>10</sup>N. J. Trappeniers and W. Mandema, Physica **32**, 1170 (1966).

<sup>11</sup>C. W. Garland and R. Renard, J. Chem. Phys. **44**, 1130 (1966).

<sup>12</sup>C. W. Garland and B. B. Weiner, Phys. Rev. B **3**, 1634 (1971).

<sup>13</sup>C. W. Garland and R. J. Pollina, J. Chem. Phys. **58**, 5002 (1973).

<sup>14</sup>R. B. Griffiths, Phys. Rev. Lett. **24**, 715 (1970).

<sup>15</sup>E. K. Riedel and F. J. Wegner, Phys. Rev. Lett. **29**, 349 (1972).

<sup>16</sup>A. Hankey, H. E. Stanley, and T. S. Chang, Phys. Rev. Lett. **29**, 278 (1972).

<sup>17</sup>F. Harbus and H. E. Stanley, Phys. Rev. Lett. **29**, 58 (1972).

<sup>18</sup>P. J. Kortman, Phys. Rev. Lett. **29**, 1449 (1972).

<sup>19</sup>M. Blume, V. J. Emery, and R. B. Griffiths, Phys. Rev. A **4**, 1071 (1971).

<sup>20</sup>I. J. Fritz and H. Z. Cummins, Phys. Rev. Lett. **28**, 96 (1972).

<sup>21</sup>R. J. Birgeneau, W. B. Yelon, E. Cohen, and J. Makowsky, Phys. Rev. B **5**, 2607 (1972); W. B. Yelon and R. J. Birgeneau, *ibid.* **5**, 2615 (1972).

<sup>22</sup>W. P. Wolf, B. Schneider, D. P. Landau, and B. E.

- Keen, Phys. Rev. B 5, 4472 (1972).
- <sup>23</sup>C. M. Lai and T. A. Kitchens (unpublished).
- <sup>24</sup>G. Goellner and H. Meyer, Phys. Rev. Lett. 26, 1534 (1971).
- <sup>25</sup>I. S. Jacobs and P. E. Lawrence, Phys. Rev. 164, 866 (1967).
- <sup>26</sup>L. T. Todd, Jr., MIT Crystal Physics Laboratory Technical Report No. 14 (unpublished).
- <sup>27</sup>G. H. Goldschmidt and D. G. Hurst, Phys. Rev. 83, 88 (1951). H. A. Levy and S. W. Peterson, Phys. Rev. 86, 766 (1952).
- <sup>28</sup>K. N. Trueblood, Acta Cryst. 9, 359 (1956); W. J. A. M. Peterse and J. H. Palm, *ibid.* 20, 147 (1966).
- <sup>29</sup>W. B. Yelon and D. E. Cox, Solid State Commun. 11, 1011 (1972).
- <sup>30</sup>H. Umabayashi, G. Shirane, B. C. Frazer, and W. B. Daniels, Phys. Rev. 165, 688 (1968).
- <sup>31</sup>A. Tucciarone, H. Y. Lau, L. M. Corliss, A. Delapalme, and J. M. Hastings, Phys. Rev. B 4, 3206 (1971).
- <sup>32</sup>M. Lax (private communication).
- <sup>33</sup>The notation in use,  $\psi$  for the order parameter and  $g$  here, is in accord with Griffiths' proposed notation for TCP's. R. B. Griffiths, Phys. Rev. B 7, 545 (1972).
- <sup>34</sup>M. E. Fisher and R. J. Burford, Phys. Rev. 156, 587 (1967).
- <sup>35</sup>R. J. Birgeneau, J. Skalyo, Jr., and G. Shirane, Phys. Rev. B 3, 1736 (1971).
- <sup>36</sup>M. Lambert (private communication).
- <sup>37</sup>Y. Yamada, M. Mori, and Y. Noda, J. Phys. Soc. Jap. 32, 1565 (1972); A. Huller, Z. Phys. 254, 1757 (1972).
- <sup>38</sup>R. Stevenson, J. Chem. Phys. 34, 1757 (1961).
- <sup>39</sup>R. B. Griffiths, *Critical Phenomena in Alloys, Magnets, and Superconductors*, edited by R. E. Mills, E. Ascher, and R. I. Jaffee (McGraw-Hill, New York, 1971), p. 377.
- <sup>40</sup>A line of tricritical points has recently been observed as a function of pressure in  $\text{FeCl}_2$  and  $\text{FeBr}_2$ ; D. Bloch and C. Vettier (private communication).
- <sup>41</sup>R. B. Griffiths and J. C. Wheeler, Phys. Rev. A 2, 1047 (1970).
- <sup>42</sup>W. B. Yelon, Proceedings of the NATO A.S.I. Anharmonic Lattices, Structural Transitions and Melting, 1973 (unpublished).
- <sup>43</sup>P. Schofield, Phys. Rev. Lett. 22, 606 (1969).